Report on the Common Shielding Activities: Beam Guide Shielding within the LOS

T. Randriamalala
Jülich Centre for Neutron Science, Forschungszentrum Jülich GmbH

December 19, 2018

Contents

Abstract

This reports the neutronics calculations that have been carried out for the ESS common shielding project. It aimed at the establishment of an optimized configuration using Monte Carlo particle transport simulations. The optimization activities tend to modify a predefined configuration through radiation shielding effectiveness studies and activation analysis. Referring to the key parameters that drive the current calculation, only the radiation background has not been studied and is therefore not included in this report. The calculations were realized considering the DREAM and TREX instruments. The components that have been investigated include the beam guide shielding and the chopper pit within the LOS. PHITS [1] and DCHAIN-SP [2] were used for the particle transport simulations and for the activation analysis, respectively.

1 General Consideration and Source Term

The calculations were based on the assumption that the accelerator operates with the 5MW power and the proton beam has an energy of 2GeV. That corresponds to 1.56×10^{16} protons per second, the factor with which the source terms have been normalized. Indeed, in order to optimize the simulation running time, ST_{23}, source terms at x=23m[1] position were considered for the current calculations and for both instruments. Their compilations have been done in 2 steps: the definition of the ST_2, the 2m source term, from the $p+W$ spallation simulations, followed by the transport simulations using the ST_2 being established, in which the neutron tracks were dumped on a surface at the ST_{23} target position. The choice of the ST_{23} position is related to the feasibility of the ST_2 validation at this position and the integration of the bunker feed-through collimation within the simulation setup. A comparison of the neutron energy spectra obtained from simulations using $p+W$ and ST_2 at x$\simeq$23m is presented in Figure 12 in A.

As mentioned earlier, the source term was derived from the property of neutron tracks dumped on a surface located at the position of interest. Depending on their energies, E_n, neutron tracks have been classified as good if $E_n \leq$300 meV, or bad, otherwise. The good neutrons were used to determine the optics parameters of the beam guide. Consequently, they can be accurately characterized with McStas [3]. They are supposed to be fully transported to the sample location and therefore can be omitted in the source term description. Indeed, in particular for the region within the LOS, the good neutrons would only affect the shielding calculations at the focusing part where the contribution of the secondary photons might prevail. If they are escaping the guide material, they will be completely absorbed by the borated material surrounding the guide. Hence, the bad neutrons drive the configuration of the shielding structure around the beam guide and thus, has only been considered for ST_{23}.

The properties of the dumped neutron tracks at the ST_{23} position for the two considered instruments are shown in Figure 1. The corresponding integrated flux obtained from the simulations are 9.41×10^7 and 2.44×10^7 for TREX and DREAM, respectively. The ST_{23} input file used for the calculations related to DREAM can be found in Listing 1 in A.

The shielding structure must target at the accepted radiation dose level for supervised area. With the safety factor of 2, simulations must show that a radiation dose rate of 1.5 μSv/h is achieved with any shielding component. The Flux-to-Dose (FTD) conversion factors tabulated in [4] were used. A logarithmic interpolation was applied for non-tabulated energy values.

The geometry model implemented in the simulation has been compiled using the CombLayer code [5].

[1]The coordinate system adopted for the simulations shares the same origin as the Target Coordinate System (TCS) but the x- and y-axis are oriented parallel to those of the Instrument Source Coordinate System (ISCS), respectively.The x-direction corresponds to the beam direction.

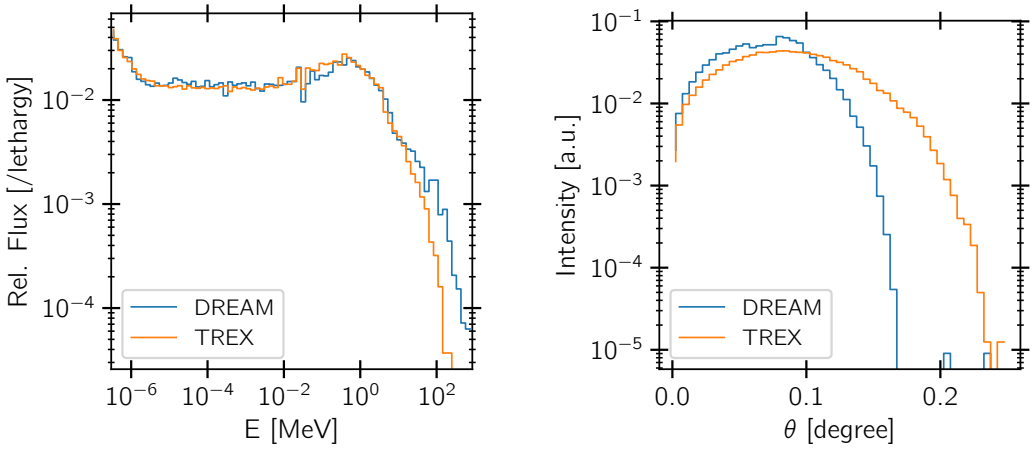

(a) (b)

Figure 1: (a) Energy and (b) angular divergence distributions of neutron tracks dumped on a surface located at x=23m that were used to derive the ST_{23} source terms.

2 Common Shielding Configuration

The simulations for the beam guide shielding outside the bunker area have been conducted based on the entire beam guide of DREAM and a part of that of TREX. The chopper pit optimization calculations have been focused only the first chopper pit after the bunker wall of TREX. Indeed, taking into account the position of all chopper pits at ESS, it is considered to be the one which would suffer the most from the neutron radiations.

A description of the master layouts proposed by S. Kudumovic for both components can be found in [6]. The main beam guide shielding will be interfaced to the bunker wall using a different configuration. The main structure will start at the smallest distance possible from the beam guide. An inner space of 44cm width was proposed and has been applied for the current calculations. Identical blocks are planed to be implemented in the shielding structure for both D01/D03 and E03 regions. However, their configurations differ due to the grounding level. Since the out-bunker beam guides of DREAM and TREX (up to the chopper pit) are located in the D01/D03 building, the calculations were focused on the shielding part of the instrument in that region.

2.1 Beam Guide Shielding

Outside the bunker, DREAM has a straight beam guide with about 6cm×6cm cross section up to the focusing guide which starts at x=59m. The beam focus has a elliptic profile ending with a cross section dimension of about 4cm×4cm at the entrance of the experimental cave. The guide substrate is made of glass. The TREX beam guide uses a borosilicate glass as a substrate material. It is bended on the horizontal plane with a curvature radius of 12km. It loses the LOS at about x=76m. Within the LOS, the beam guide has an elliptic profile on the vertical direction and has a cross section dimension going from 6cm×8cm

to 6cm×8.5cm. The substrate materials used for the bunker feed-trough are copper and aluminum for DREAM and TREX, respectively. The definition of all materials used in the simulations can be seen in B.

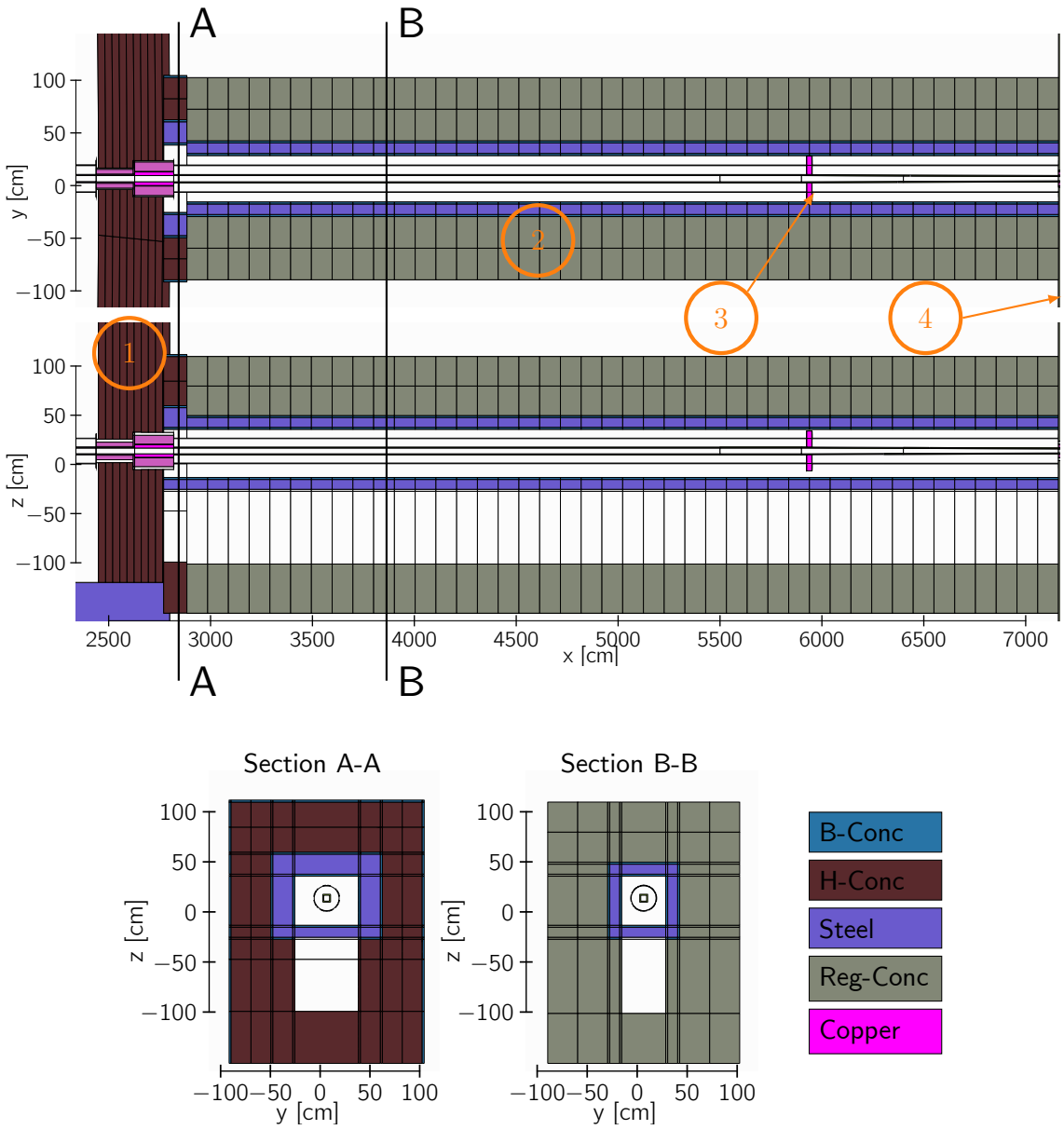

Figure 2: Schematic layout of the typical simulated geometry. It includes the following main parts: (1) the bunker wall, (2) the beam guide shielding structure, (3) a collimator (here, made of copper, but mostly considered as void) and (4) the experimental cave wall. This configuration is the one implemented in the simulations related to the DREAM instrument. On the legend at the lower rightmost of the picture, B-Conc, H-Conc and Reg-Conc stand for borated, heavy and regular concretes, respectively. The color material code will be kept through the report.

A typical problem geometry that has been implemented in the simulation is described by Figure 2. Actually, the layout of the shielding structure on this figure corresponds to the optimized configuration for both instruments. Basically, it consists of a steel inner layer and a concrete outer layer. Regular concrete is used almost everywhere except the part interfacing the bunker wall where the heavy concrete is used instead.

Modifications have been made to the proposed initial configuration after having simulated different geometries iteratively. Indeed, the simulations have highlighted the need to have a lower steel plate. In this regard, simulations were carried out on the basis of a shielding configuration with 10 cm borated concrete, 10cm steel and 50cm regular concrete. A schematic layout of the considered configuration is shown on Figure 3(a). The simulation results are given by the plots on the same figure. As illustrated by Figure 3(b), the neutrons escape the beam guide mostly from the lower side and bottom parts of the shielding structure. Those neutrons still have a non-negligible fraction of high energy neutrons (neutrons with energy greater than 1MeV). The later contribute to the about 45% of the 4.5μSv/h total dose rate. Such neutrons could not be attenuated only by the regular concrete. A steal layer is needed at the bottom part of the structure. It has to be noted that the dose rate of 1.5μSv/h could be reached outside from the top of the shielding with a concrete layer of 60cm thickness.

Another modification that is worth to be considered is the addition of an outer layer of borated concrete for the part of the shielding connected to the bunker wall. As shown in Figure 4, neutrons (mostly moderated) are leaking out from the structure. A total neutron dose rate of 5.2μSv/h was estimated from the simulations. The neutrons with energy less than 1MeV carry the 98% of the total dose rate. Based on the simulations, a borated concrete layer of 2mm thickness will bring the dose rate to less than 1.5μSv/h.

The last modification that should be taken into account consists on interposing a thin layer of borated concrete between the steel and the outer concrete layers. It prevents, by capture, most of the neutrons thermalized and/or moderated by the steel to reach the concrete layer and vice versa. It also contributes to the reduction of the total dose rate outside the shielding. Figure 5 compares the neutron spectra outside the shielding structure connected to the bunker wall without the outermost boron layer. A factor of 1.5 reduction of the dose rate is observed when the borated concrete layer is considered, leading to a dose rate of about 3.5μSv/h. But the main purpose of the borated layer is connected to the activation of the concrete layer. The corresponding analysis will be addressed in Section 3.

The consideration the modifications mentioned leads to the configuration shown in Figure 2. The corresponding neutron dose maps for DREAM and TREX beam guide shielding are plotted in Figure 6. For the TREX case, only the part before the first chopper pit which suffers the most from the neutron radiations, is shown. For the non focusing beam part of the guide, the neutron radiations contribute to more than 90% of the total radiation dose rate entering the shielding structure. This corresponds to the entire within the LOS part for TREX and the beam guide part up to x=59m for DREAM. Only at the edge the focusing beam part of DREAM, before the entrance the experimental cave that the photon dose prevails according the calculations carried out by R. Kolevatov (see Figure 13 in C).

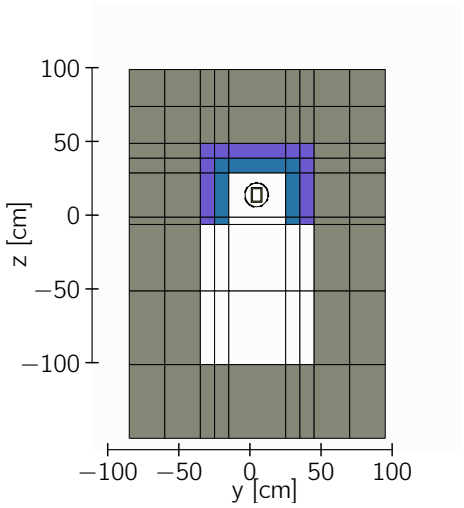

(a)

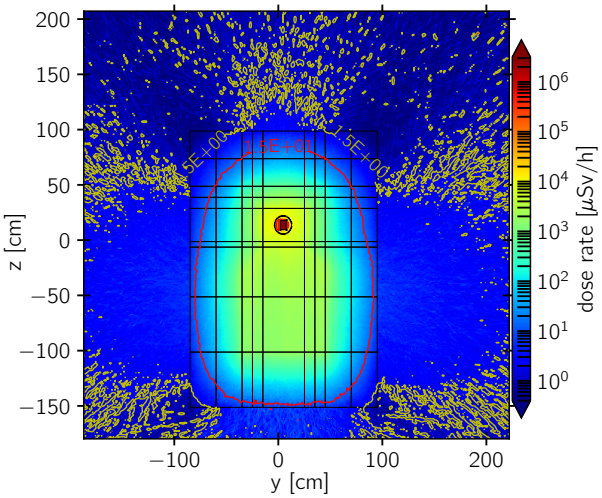

(b)

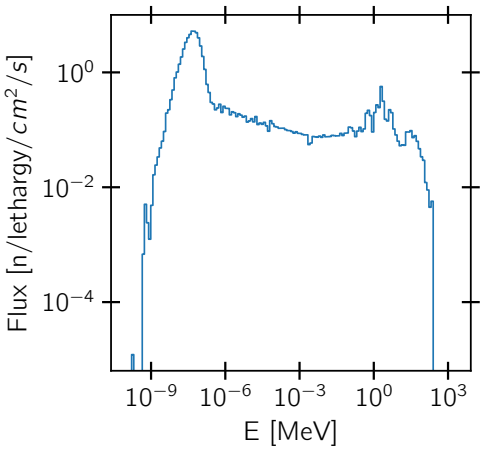

(c)

Figure 3: (a) yz cross section layout at x=3570cm of the simulated geometry, (b) the neutron dose rate map (c) the spectrum of the neutrons exiting the structure from one of the sides. The simulation has been performed with the TREX instrument and the considered configuration is described in the text.

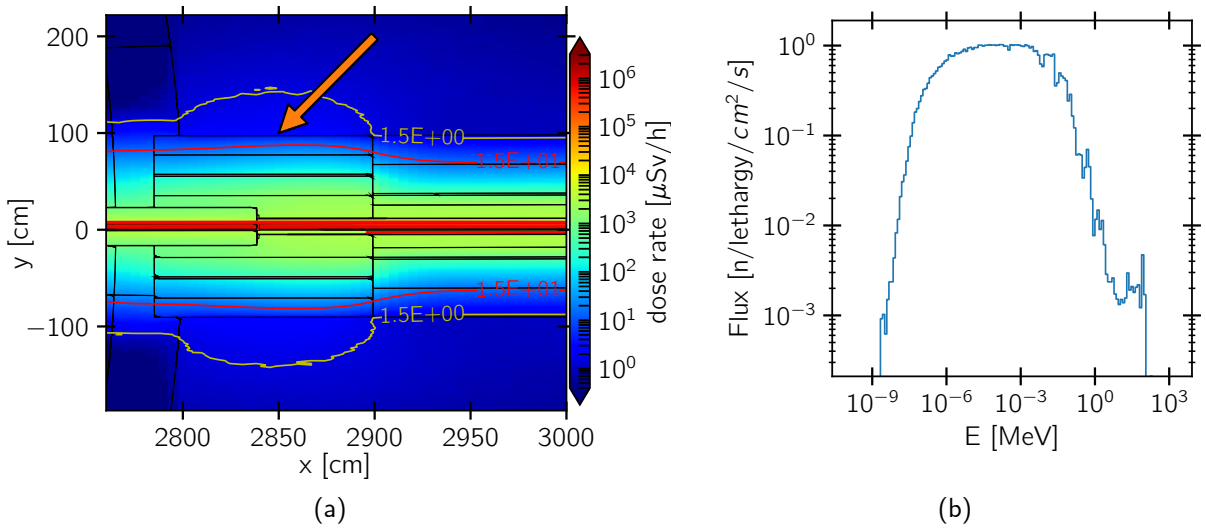

Figure 4: (a) Dose rate and (b) energy distributions of the neutrons for the shielding part connected to the bunker wall. The spectrum on the right has been obtained from the neutrons tallied at the position indicated by the orange arrow.

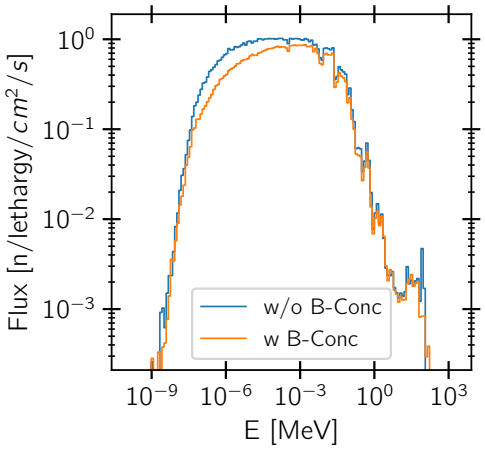

Figure 5: Energy spectra of neutrons outside the part of the shielding connected to the bunker wall for the configurations with and without borated concrete layer between the steel and the outer concrete layers.

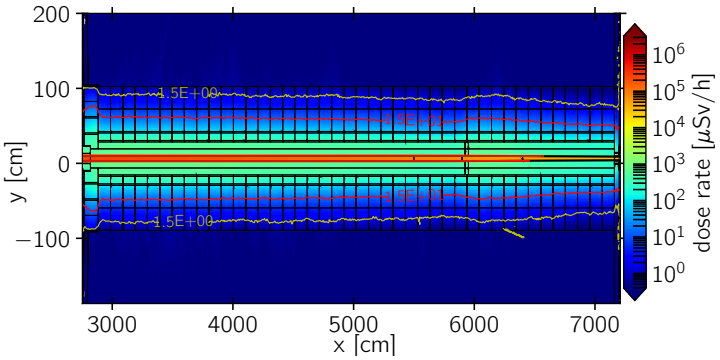

(a) xy-distribution (DREAM)

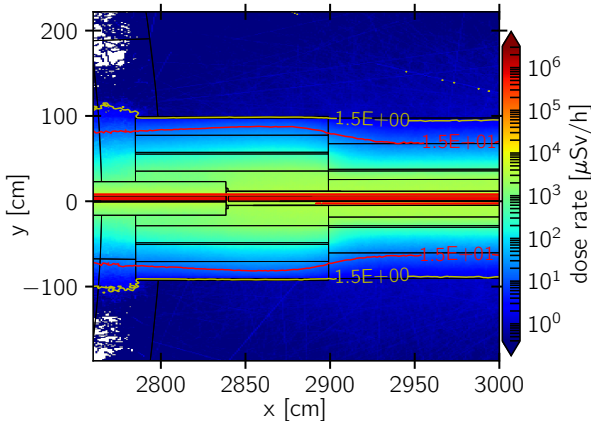

(b) xy-distribution (TREX)

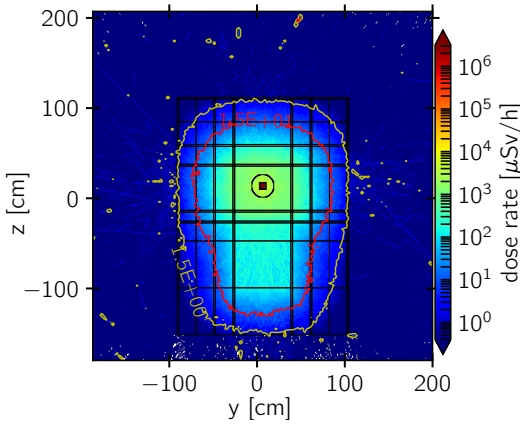

(c) yz-distribution at x≃28.5m

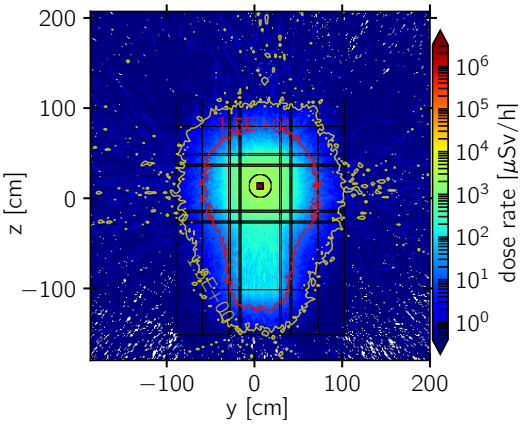

(d) yz-distribution at x≃59m (DREAM)

Figure 6: Neutron dose rate distribution corresponding to the shielding structure shown in Figure 2 established by the neutronics calculations.

2.2 Chopper Pit

Within the LOS, TREX has two bandwidth choppers located at x=32m and x=40m ,respectively. In the simulations chopper materials have been omitted and gaps have been used instead. Worse case scenarios can be mimicked therewith.

The neutron dose rate distribution corresponding to the initial chopper pit configuration is shown in Figure 7(a). The dose rate level outside the pit is still greater than 1.5μSv/h due to neutrons escaping at its rear side. On the outer surface of that side, the spectrum of neutrons for the first chopper pit, a indicated by the orange arrow on Figure 7(a), is plotted in Figure 7(b). It corresponds to the typical spectrum of neutrons leaking that side of the pit. However, the integrated flux, and thus the dose rate, decreases with the distance to the source as dose rate levels of 4.2μSv/h and 3.7μSv/h are obtained for the first and second chopper pits, respectively.

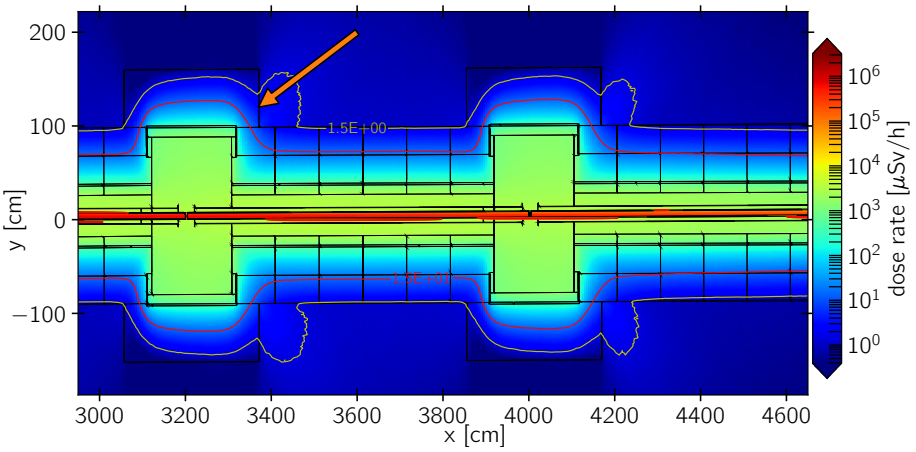

(a)

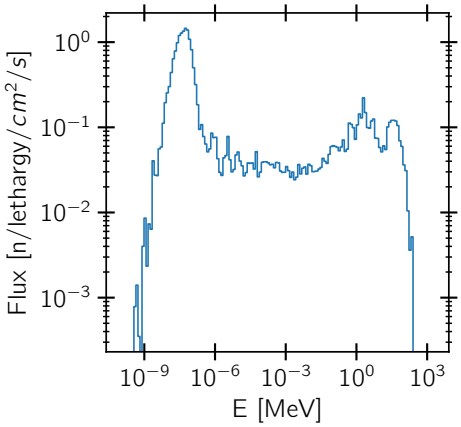

(b)

Figure 7: (a) Neutron dose rate distribution and (b) energy distribution of the neutrons escaping the chopper pit at for the position indicated by the orange arrow on the left figure.

Config. Type	Thickness [cm] Steel	Concrete	Dose Rate [μSv/h] E_n <1MeV	$E_n \geq$ 1MeV
I	10	52	1.6	2.6
	10	52†	1.9	2.4
	20	52	1.6	2.4
	20	80	1.5	2.3
II	10	60	1.4	1.7
	10	80	1.3	1.6
III	10	52	1.3	0.9
	10	152	1.0	0.6

Table 1: Neutron dose at the rear side of the first chopper of TREX for (I) configurations based on the initial one, (II) configurations with the steel layer covering the inner rear side and (III) configurations with a copper collimator at the entrance of chopper pit and the inner rear side fully covered by the steel. (†) Heavy concrete was used instead of regular concrete.

Several configurations have been simulated in order to identify the leaking path for the neutrons. And based on that, an optimal configuration of the chopper pit can be designed. Table 1 summarizes the results from different simulations in term of the dose rate level at the rear side of the first chopper.

Referring to Table 1, the dose rate level required by the safety regulation can only be achieved with the second configuration of type III, which has the steel layer covering the entire rear side, a collimator placed at the entrance and the concrete layer thickened up to 152cm. A schematic layout of a such configuration implemented within the simulated geometry and the corresponding neutron dose rate distribution are shown in Figure 8 and Figure 9, respectively.

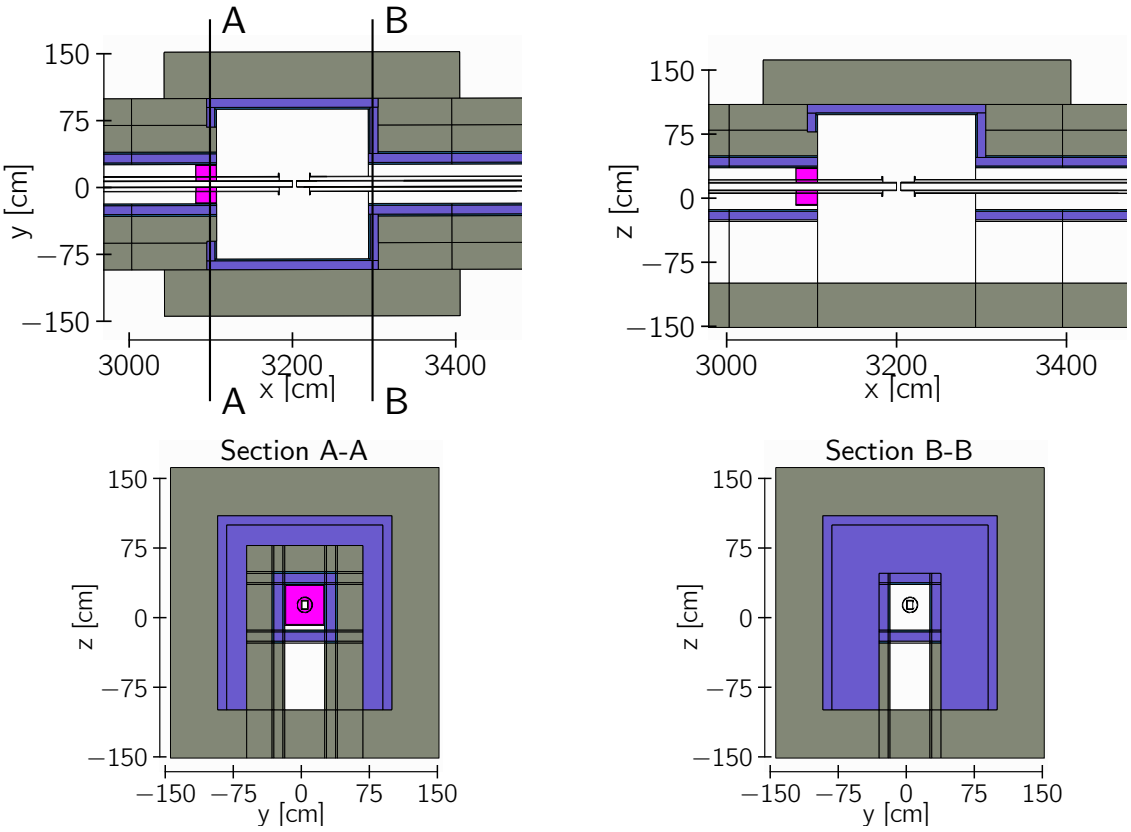

Figure 8: Layout of the first chopper pit of TREX implemented in simulation which satisfies the target dose rate level for the shielding calculation.

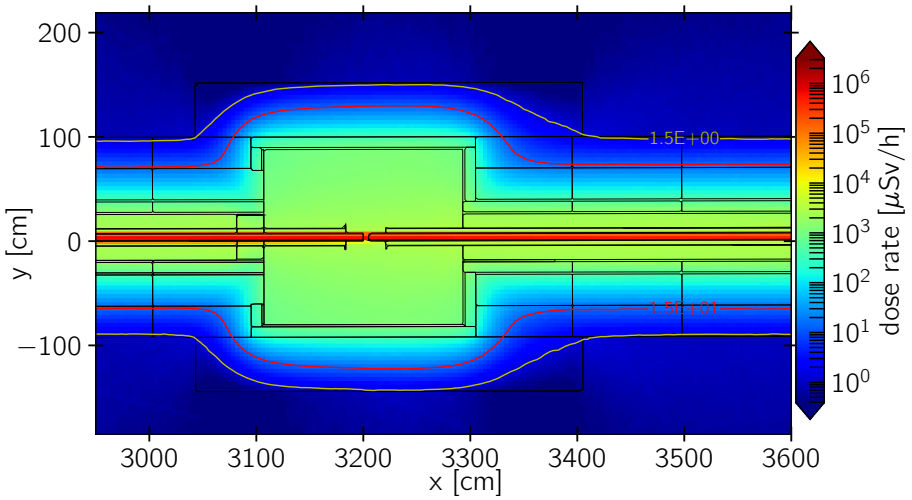

Figure 9: Neutron dose rate distribution at the first chopper pit of TREX using the configuration shown in Figure 8.

3 Activation

The main purpose of the activation analysis is to identify the role of the inner and intermediate borated concrete layers within the shielding structure. Therefore, the comparison in term of activation has been carried out for two different shielding structure with and without the borated concrete layers at all. The simulations were based on the TREX geometry setup up to the first chopper. A direct illumination of the inner shielding surface by the source can be obtained with this setup.

Ten years continuous irradiation has been considered. The graph showing the decay of the contact dose rate with the cooling time is plotted in Figure 10. The residual activity with the configuration containing borated concrete is a factor 2 lower compared to that of obtained with the other configuration. 12 hours cooling duration would be required for the later to reach the dose level of the first configuration right after the end of the irradiation. After 5 days cooling period, the activities of the shielding and chopper pit are reduced to the potassium-40 in the concrete.

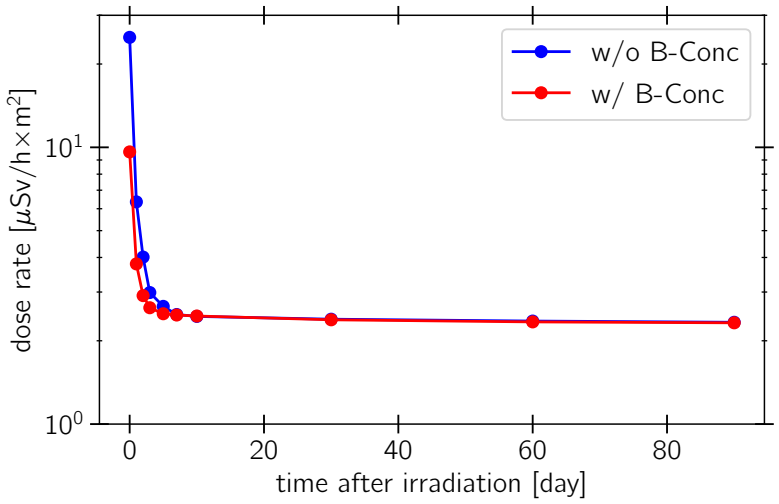

Figure 10: Dose rate decay as a function of the cooling time for the with and without borated concrete layers configuration.

The dose rate maps of the emitted photon radiation after the activation simulation for different geometry and cooling time are shown in Figure 11. The implementation of the borated concrete within the shielding structure would allow the chopper pit region to be accessible right after the end of the irradiation.

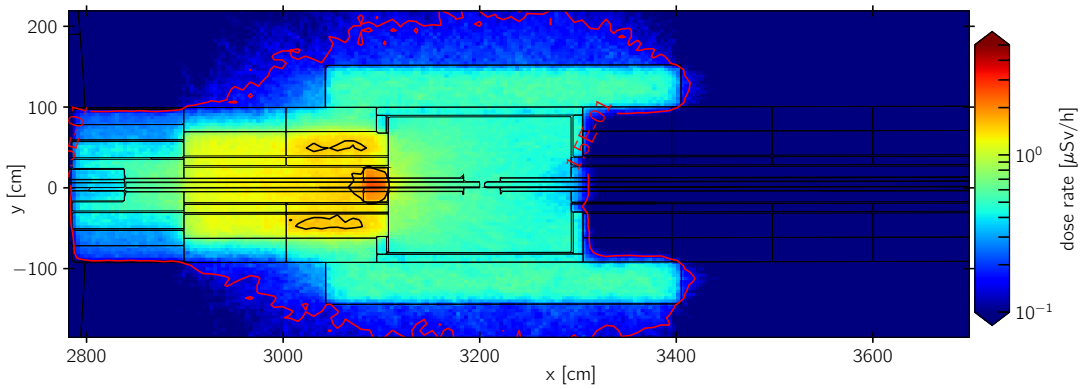

(a) with B-Conc, Cooling duration = 0 day

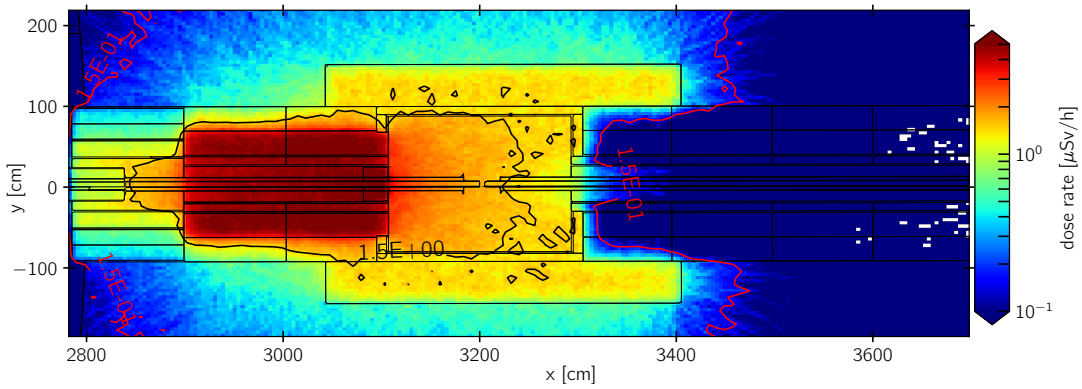

(b) without B-Conc, Cooling duration = 0 day

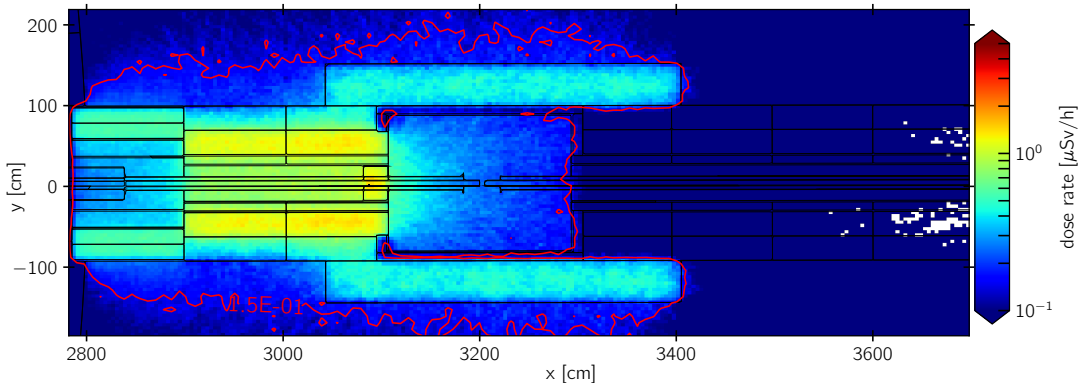

(c) without B-Conc, Cooling duration = 1 day

Figure 11: Photon dose rate distribution for different simulation configurations.

4 Summary Tables

Layer N.	Material	Thickness [cm] left	right	top	bottom
I. Shielding part connected to the bunker wall					
1	B-Concrete	2	2	2	2
2	Steel	20	20	20	10
3	B-Concrete	2	2	2	2
4	H-Concrete	40	40	50	-
5	B-Concrete	2	2	2	-
II. Main shielding part					
1	B-Concrete	2	2	2	2
2	Steel	10	10	10	10
3	B-Concrete	2	2	2	2
4	Reg-Concrete	60	60	60	-

Table 2: Shielding layer configuration inside out.

Layer N.	Material	Thickness [cm] left	right	top	bottom	front	rear
1	B-Concrete	2	2	2	-	2	2
2	Steel	10	10	10	-	10	10
3	Reg-Concrete	60	60	60	-	52	152

Table 3: Chopper pit layer configuration inside out. Steel layer covers partially the front side.

A Additional Material - Source Term

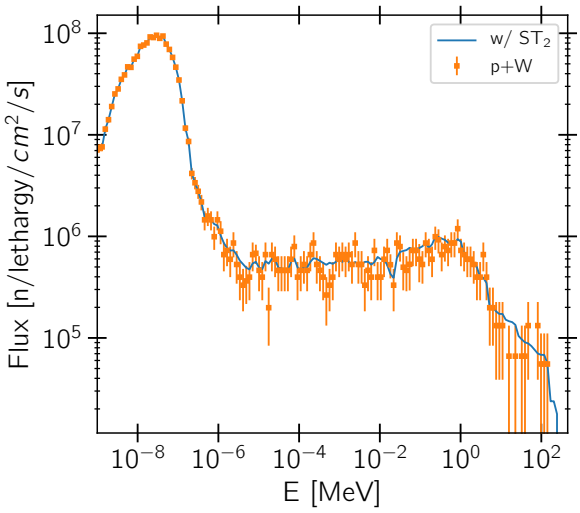

Figure 12: Energy spectra of neutrons at x≃23m obtained from simulations using $p + W$ and ST_2 as sources.

Listing 1: Source term used for the beam guide shielding simulations for DREAM.

```
[ Source ]
totfact   =  8.278055153E+08

### On-Beam with div. less than 0.2 deg
<source>  =  9.927687250E-01
proj  =  neutron
s-type  =  5
x0  =  -2.930E+00
x1  =  2.930E+00
y0  =  -2.930E+00
y1  =  2.930E+00
z0  =  -5.000E-04
z1  =  5.000E-04
dir   =  data
a-type  =  11
na  =  50
   0.00000E+00   1.12200E-03
   3.34805E-03   3.56506E-03
   6.69609E-03   5.69143E-03
   1.00441E-02   8.25212E-03
   1.33922E-02   1.06680E-02
   1.67402E-02   1.28125E-02
   2.00883E-02   1.55451E-02
   2.34363E-02   1.78525E-02
   2.67844E-02   2.04222E-02
   3.01324E-02   2.22952E-02
   3.34805E-02   2.51183E-02
   3.68285E-02   2.75976E-02
   4.01766E-02   2.66203E-02
   4.35246E-02   2.92444E-02
   4.68726E-02   3.20675E-02
   5.02207E-02   3.31714E-02
   5.35687E-02   3.47367E-02
   5.69168E-02   3.52253E-02
   6.02648E-02   3.18413E-02
   6.36129E-02   3.26918E-02
   6.69609E-02   3.42934E-02
   7.03090E-02   3.48815E-02
   7.36570E-02   3.44743E-02
   7.70051E-02   3.59311E-02
   8.03531E-02   4.42737E-02
   8.37012E-02   4.27265E-02
   8.70492E-02   4.18759E-02
   9.03973E-02   3.87995E-02
   9.37453E-02   3.83742E-02
   9.70933E-02   3.46915E-02
   1.00441E-01   2.78419E-02
   1.03789E-01   2.63217E-02
   1.07137E-01   2.27929E-02
   1.10486E-01   2.00965E-02
   1.13834E-01   1.82415E-02
   1.17182E-01   1.60790E-02
   1.20530E-01   1.38259E-02
   1.23878E-01   1.09938E-02
   1.27226E-01   9.24745E-03
   1.30574E-01   7.56445E-03
   1.33922E-01   5.65524E-03
   1.37270E-01   4.25274E-03
   1.40618E-01   3.62840E-03
   1.43966E-01   2.51545E-03
   1.47314E-01   1.52013E-03
   1.50662E-01   1.32106E-03
   1.54010E-01   6.33387E-04
   1.57358E-01   3.52887E-04
   1.60706E-01   1.62871E-04
   1.64054E-01   9.04838E-05
   1.67402E-01
e-type  =  1
```

```
ne  =  -69
   3.00167E-07   6.04348E-02
   4.11560E-07   6.50792E-02
   5.64291E-07   6.24990E-02
   7.73701E-07   6.12089E-02
   1.06082E-06   5.78259E-02
   1.45450E-06   5.76539E-02
   1.99427E-06   5.53317E-02
   2.73435E-06   5.07159E-02
   3.74907E-06   5.00565E-02
   5.14036E-06   5.18054E-02
   7.04796E-06   5.07733E-02
   9.66348E-06   5.06299E-02
   1.32496E-05   5.92594E-02
   1.81666E-05   5.65358E-02
   2.49083E-05   5.38695E-02
   3.41518E-05   5.21781E-02
   4.68257E-05   5.25508E-02
   6.42028E-05   4.89671E-02
   8.80287E-05   5.42136E-02
   1.20696E-04   4.96552E-02
   1.65487E-04   5.10886E-02
   2.26900E-04   5.16907E-02
   3.11103E-04   4.23158E-02
   4.26554E-04   5.33248E-02
   5.84850E-04   4.95405E-02
   8.01890E-04   5.49016E-02
   1.09947E-03   5.02859E-02
   1.50749E-03   5.33248E-02
   2.06693E-03   4.57275E-02
   2.83397E-03   4.71323E-02
   3.88566E-03   5.22354E-02
   5.32764E-03   4.93111E-02
   7.30474E-03   5.12606E-02
   1.00156E-02   5.08879E-02
   1.37324E-02   5.46149E-02
   1.88285E-02   5.89153E-02
   2.58158E-02   6.13522E-02
   3.53961E-02   4.35773E-02
   4.85317E-02   6.10369E-02
   6.65420E-02   6.00334E-02
   9.12359E-02   6.13236E-02
   1.25094E-01   6.11515E-02
   1.71516E-01   7.06124E-02
   2.35167E-01   8.36282E-02
   3.22438E-01   8.22808E-02
   4.42095E-01   8.61798E-02
   6.06158E-01   8.79286E-02
   8.31105E-01   7.78657E-02
   1.13953E+00   7.14438E-02
   1.56241E+00   6.57960E-02
   2.14223E+00   5.43283E-02
   2.93722E+00   4.85657E-02
   4.02723E+00   4.01656E-02
   5.52175E+00   2.99307E-02
   7.57088E+00   1.89791E-02
   1.03805E+01   1.50227E-02
   1.42327E+01   1.33312E-02
   1.95145E+01   1.20698E-02
   2.67563E+01   1.01776E-02
   3.66857E+01   8.94481E-03
   5.02999E+01   5.30381E-03
   6.89663E+01   5.99188E-03
   9.45599E+01   5.64784E-03
   1.29651E+02   2.86693E-03
   1.77765E+02   2.75225E-03
   2.43735E+02   1.08943E-03
   3.34185E+02   7.45401E-04
   4.58202E+02   2.58023E-04
   6.28243E+02   2.29354E-04
   8.61385E+02
trcl  =  2.315E+03  6.530E+00  1.370E+01
      0.000E+00  0.000E+00  1.000E+00
      0.000E+00 -1.000E+00  0.000E+00
      1.000E+00  0.000E+00  0.000E+00  1

### On-Beam with div. greater than 0.2 deg
<source>  =  5.524514472E-03
proj  =  neutron
s-type  =  5
x0  =  -2.930E+00
x1  =  2.930E+00
y0  =  -2.930E+00
y1  =  2.930E+00
z0  =  -5.000E-04
z1  =  5.000E-04
dir  =  data
a-type  =  11
na  =  40
   2.09343E-01   1.78862E-02
   2.38159E+00   2.60163E-02
   4.55384E+00   2.43902E-02
   6.72610E+00   1.30081E-02
   8.89835E+00   2.92683E-02
   1.10706E+01   1.30081E-02
   1.32428E+01   3.08943E-02
   1.54151E+01   1.62602E-02
   1.75874E+01   2.92683E-02
   1.97596E+01   2.60163E-02
   2.19319E+01   2.76423E-02
   2.41041E+01   2.60163E-02
   2.62764E+01   3.73984E-02
   2.84486E+01   1.78862E-02
   3.06209E+01   2.11382E-02
   3.27931E+01   2.76423E-02
   3.49654E+01   3.25203E-02
   3.71376E+01   1.95122E-02
   3.93099E+01   3.25203E-02
   4.14821E+01   3.73984E-02
   4.36544E+01   3.57724E-02
   4.58266E+01   1.62602E-02
   4.79989E+01   3.73984E-02
   5.01711E+01   2.27642E-02
   5.23434E+01   3.25203E-02
   5.45156E+01   2.11382E-02
   5.66879E+01   2.76423E-02
   5.88601E+01   3.25203E-02
   6.10324E+01   1.78862E-02
   6.32046E+01   2.76423E-02
   6.53769E+01   2.76423E-02
   6.75491E+01   3.73984E-02
   6.97214E+01   1.62602E-02
   7.18936E+01   2.92683E-02
   7.40659E+01   1.78862E-02
   7.62381E+01   2.60163E-02
   7.84104E+01   1.95122E-02
   8.05826E+01   2.43902E-02
   8.27549E+01   1.62602E-02
   8.49271E+01   8.13008E-03
   8.70994E+01
e-type  =  1
ne  =  -69
   3.02014E-07   4.77877E-02
   4.10224E-07   3.18585E-02
   5.57207E-07   2.12390E-02
   7.56853E-07   5.84072E-02
```

```
   1.02803E-06   4.77877E-02
   1.39638E-06   2.12390E-02
   1.89669E-06   3.18585E-02
   2.57628E-06   1.59292E-02
   3.49935E-06   5.30974E-02
   4.75316E-06   3.71682E-02
   6.45621E-06   1.59292E-02
   8.76946E-06   3.71682E-02
   1.19115E-05   2.12390E-02
   1.61794E-05   2.65487E-02
   2.19765E-05   2.65487E-02
   2.98506E-05   5.30974E-03
   4.05460E-05   1.59292E-02
   5.50736E-05   2.65487E-02
   7.48064E-05   2.65487E-02
   1.01609E-04   1.06195E-02
   1.38016E-04   5.30974E-02
   1.87467E-04   3.18585E-02
   2.54636E-04   7.96461E-02
   3.45871E-04   4.77877E-02
   4.69796E-04   1.59292E-02
   6.38123E-04   3.18585E-02
   8.66762E-04   2.12390E-02
   1.17732E-03   3.71682E-02
   1.59915E-03   4.77877E-02
   2.17213E-03   6.37169E-02
   2.95040E-03   5.84072E-02
   4.00752E-03   3.71682E-02
   5.44340E-03   3.71682E-02
   7.39377E-03   4.24779E-02
   1.00429E-02   2.12390E-02
   1.36413E-02   2.12390E-02
   1.85290E-02   3.71682E-02
   2.51679E-02   8.49559E-02
   3.41855E-02   7.96461E-02
   4.64340E-02   9.55754E-02
   6.30713E-02   1.27434E-01
   8.56696E-02   7.43364E-02
   1.16365E-01   1.43363E-01
   1.58058E-01   1.53983E-01
   2.14690E-01   1.22124E-01
   2.91613E-01   1.16814E-01
   3.96098E-01   1.32744E-01
   5.38019E-01   1.22124E-01
   7.30790E-01   1.38053E-01
   9.92631E-01   8.49559E-02
   1.34829E+00   7.43364E-02
   1.83138E+00   7.43364E-02
   2.48756E+00   7.96461E-02
   3.37885E+00   8.49559E-02
   4.58948E+00   1.06195E-02
   6.23388E+00   3.71682E-02
   8.46747E+00   1.59292E-02
   1.15014E+01   1.06195E-02
   1.56223E+01   3.18585E-02
   2.12197E+01   2.65487E-02
   2.88227E+01   1.06195E-02
   3.91498E+01   1.59292E-02
   5.31771E+01   5.30974E-03
   7.22303E+01   2.65487E-02
   9.81103E+01   1.59292E-02
   1.33263E+02   0.00000E+00
   1.81011E+02   0.00000E+00
   2.45867E+02   0.00000E+00
   3.33961E+02   5.30974E-03
   4.53618E+02
trcl  =  2.315E+03  6.530E+00  1.370E+01
     0.000E+00  0.000E+00  1.000E+00
     0.000E+00 -1.000E+00  0.000E+00
     1.000E+00  0.000E+00  0.000E+00  1

### Off-beam tracks
<source>  =  1.706760568E-03
s-type  =  22
proj  =  neutron
dir  =  data
a-type  =  11
na  =  90
   2.72351E+00   1.57895E-02
   3.66743E+00   1.57895E-02
   4.61135E+00   2.10526E-02
   5.55526E+00   1.57895E-02
   6.49918E+00   5.26316E-03
   7.44310E+00   1.57895E-02
   8.38701E+00   0.00000E+00
   9.33093E+00   1.05263E-02
   1.02748E+01   1.05263E-02
   1.12188E+01   1.57895E-02
   1.21627E+01   5.26316E-03
   1.31066E+01   1.05263E-02
   1.40505E+01   0.00000E+00
   1.49944E+01   1.05263E-02
   1.59383E+01   1.57895E-02
   1.68823E+01   2.10526E-02
   1.78262E+01   2.10526E-02
   1.87701E+01   0.00000E+00
   1.97140E+01   2.10526E-02
   2.06579E+01   1.57895E-02
   2.16018E+01   2.10526E-02
   2.25458E+01   1.57895E-02
   2.34897E+01   1.05263E-02
   2.44336E+01   0.00000E+00
   2.53775E+01   1.05263E-02
   2.63214E+01   5.26316E-03
   2.72653E+01   1.05263E-02
   2.82093E+01   2.63158E-02
   2.91532E+01   1.05263E-02
   3.00971E+01   5.26316E-03
   3.10410E+01   1.57895E-02
   3.19849E+01   1.05263E-02
   3.29288E+01   2.63158E-02
   3.38728E+01   2.63158E-02
   3.48167E+01   0.00000E+00
   3.57606E+01   1.05263E-02
   3.67045E+01   0.00000E+00
   3.76484E+01   2.10526E-02
   3.85923E+01   1.05263E-02
   3.95363E+01   1.05263E-02
   4.04802E+01   1.05263E-02
   4.14241E+01   2.63158E-02
   4.23680E+01   1.05263E-02
   4.33119E+01   5.26316E-03
   4.42558E+01   1.05263E-02
   4.51998E+01   1.57895E-02
   4.61437E+01   1.57895E-02
   4.70876E+01   1.57895E-02
   4.80315E+01   5.26316E-03
   4.89754E+01   5.26316E-03
   4.99193E+01   1.05263E-02
   5.08633E+01   5.26316E-03
   5.18072E+01   5.26316E-03
   5.27511E+01   1.57895E-02
   5.36950E+01   1.05263E-02
   5.46389E+01   1.05263E-02
   5.55828E+01   1.57895E-02
   5.65268E+01   0.00000E+00
```

```
   5.74707E+01   1.57895E-02
   5.84146E+01   0.00000E+00
   5.93585E+01   0.00000E+00
   6.03024E+01   1.05263E-02
   6.12463E+01   1.57895E-02
   6.21903E+01   0.00000E+00
   6.31342E+01   5.26316E-03
   6.40781E+01   1.05263E-02
   6.50220E+01   5.26316E-03
   6.59659E+01   1.57895E-02
   6.69098E+01   1.05263E-02
   6.78538E+01   5.26316E-03
   6.87977E+01   0.00000E+00
   6.97416E+01   1.57895E-02
   7.06855E+01   1.05263E-02
   7.16294E+01   5.26316E-03
   7.25733E+01   1.05263E-02
   7.35173E+01   5.26316E-03
   7.44612E+01   1.05263E-02
   7.54051E+01   1.05263E-02
   7.63490E+01   5.26316E-03
   7.72929E+01   0.00000E+00
   7.82368E+01   1.05263E-02
   7.91808E+01   1.57895E-02
   8.01247E+01   0.00000E+00
   8.10686E+01   1.57895E-02
   8.20125E+01   2.10526E-02
   8.29564E+01   1.57895E-02
   8.39003E+01   1.57895E-02
   8.48443E+01   2.10526E-02
   8.57882E+01   5.26316E-03
   8.67321E+01   2.10526E-02
   8.76760E+01
e-type  =  1
ne  =  69
   3.44399E-07   7.23591E-02
   4.60700E-07   1.80898E-02
   6.16275E-07   1.80898E-02
   8.24387E-07   5.42693E-02
   1.10278E-06   3.61796E-02
   1.47518E-06   1.80898E-02
   1.97333E-06   1.80898E-02
   2.63971E-06   3.61796E-02
   3.53113E-06   3.61796E-02
   4.72356E-06   3.61796E-02
   6.31868E-06   5.42693E-02
   8.45245E-06   5.42693E-02
   1.13068E-05   1.80898E-02
   1.51250E-05   0.00000E+00
   2.02326E-05   3.61796E-02
   2.70650E-05   7.23591E-02
   3.62047E-05   1.80898E-02
   4.84308E-05   1.80898E-02
   6.47855E-05   3.61796E-02
   8.66632E-05   3.61796E-02
   1.15929E-04   3.61796E-02
   1.55077E-04   7.23591E-02
   2.07445E-04   3.61796E-02
   2.77498E-04   1.80898E-01
   3.71208E-04   7.23591E-02
   4.96562E-04   5.42693E-02
   6.64247E-04   0.00000E+00
   8.88559E-04   0.00000E+00
   1.18862E-03   3.61796E-02
   1.59001E-03   3.61796E-02
   2.12694E-03   1.80898E-02
   2.84520E-03   3.61796E-02
   3.80600E-03   0.00000E+00
   5.09126E-03   7.23591E-02
   6.81054E-03   1.08539E-01
   9.11041E-03   1.80898E-02
   1.21869E-02   9.04489E-02
   1.63024E-02   5.42693E-02
   2.18076E-02   9.04489E-02
   2.91718E-02   9.04489E-02
   3.90230E-02   5.42693E-02
   5.22008E-02   3.61796E-02
   6.98286E-02   1.26628E-01
   9.34092E-02   5.42693E-02
   1.24953E-01   3.61796E-02
   1.67149E-01   9.04489E-02
   2.23594E-01   1.08539E-01
   2.99100E-01   0.00000E+00
   4.00103E-01   9.04489E-02
   5.35215E-01   7.23591E-02
   7.15954E-01   9.04489E-02
   9.57727E-01   7.23591E-02
   1.28114E+00   7.23591E-02
   1.71378E+00   1.62808E-01
   2.29251E+00   3.61796E-02
   3.06667E+00   5.42693E-02
   4.10227E+00   7.23591E-02
   5.48757E+00   1.08539E-01
   7.34069E+00   3.61796E-02
   9.81959E+00   1.80898E-02
   1.31356E+01   3.61796E-02
   1.75714E+01   1.80898E-02
   2.35051E+01   7.23591E-02
   3.14427E+01   0.00000E+00
   4.20606E+01   0.00000E+00
   5.62642E+01   1.80898E-02
   7.52642E+01   0.00000E+00
   1.00680E+02   9.04489E-02
   1.34680E+02   1.80898E-02
   1.80160E+02
mesh  =  xyz
x-type  =  1
nx  =  3
  -5.871E+00 -2.930E+00 2.930E+00 5.871E+00
y-type  =  1
ny  =  3
  -5.829E+00 -2.930E+00 2.930E+00 5.829E+00
z-type  =  2
nz  =  -1
zmin  =  -5.000E-04
zmax  =  5.000E-04
  1.000E+00 1.000E+00 1.000E+00
  1.000E+00 0.000E+00 1.000E+00
  1.000E+00 1.000E+00 1.000E+00
trcl  =  2.315E+03  6.530E+00  1.370E+01
     0.000E+00  0.000E+00  1.000E+00
     0.000E+00 -1.000E+00  0.000E+00
     1.000E+00  0.000E+00  0.000E+00  1
```

B Materials Definition

Listing 2: Definition of materials used in the shielding and the chopper pit. The isotope densities are expressed in atom/(barn.cm) .

```
## Material : Aluminium rho=2.64651 g/cc
  27Al      0.054381
  24Mg      0.00207
  25Mg      0.0002621
  26Mg      0.0002885
  28Si      0.000217
  48Ti      8.7e-05
  52Cr      7.8e-05
  53Cr      1e-05
  55Mn      0.000408
  56Fe      0.000214
  57Fe      5e-06
  63Cu      4e-05
  65Cu      2e-05
    Zn      0.000145

## Material : Glass rho=2.44 g/cc
  40Ca      0.002719913
  42Ca      1.815314e-05
  43Ca      3.78775e-06
  44Ca      5.852775e-05
  46Ca      1.122296e-07
  48Ca      5.246735e-06
  23Na      0.006423108
  16O       0.0430724
  28Si      0.01708774
  29Si      0.000867674
  30Si      0.0005719771

## Material : Borosilicate rho=2.23 g/cc
  28Si      0.0160107
  29Si      0.000812983
  30Si      0.000535924
  10B       0.000663275
  11B       0.00266976
  27Al      0.00361079
  16O       0.0451349

## Material: Concrete rho=2.3358 g/cc
  1H        0.00776555
  2H        1.16501e-06
  16O       0.0438499
  23Na      0.00104778
  24Mg      0.000117443
  25Mg      1.48662e-05
  26Mg      1.63528e-05
  27Al      0.00238815
  28Si      0.0158026
  32S       5.63433e-05
  39K       0.000646375
  40K       8.31725e-08
  41K       4.66459e-05
  40Ca      0.00282756
  44Ca      8.74503e-05
  54Fe      1.84504e-05
  56Fe      0.000286826
  57Fe      6.5671e-06
  58Fe      8.75613e-07

## Material: Steel rho=7.79995 g/cc
  12C        0.0001011868
  28Si       0.000295128
  50Cr       7.32761e-06
  52Cr       0.000141306
  53Cr       1.60229e-05
  54Cr       3.98844e-06
  55Mn       0.0005059338
  54Fe       0.004841401
  56Fe       0.07599964
  57Fe       0.001755163
  58Fe       0.00023358
  58Ni       0.000172218
  60Ni       6.633503e-05
  61Ni       2.881261e-06
  62Ni       9.192715e-06
  64Ni       2.339918e-06
  63Cu       0.0001166515
  65Cu       5.199313e-05

## Material: Copper rho=8.91001 g/cc
  63Cu      0.058389212
  65Cu      0.02604927

## Material: Heavy Concrete rho=3.80022 g/cc
  16O       0.03821889
  27Al      0.002111912
  28Si      0.007634835
  32S       0.0005845036
  39K       0.000640271
  40K       8.23871e-08
  41K       4.62054e-05
  40Ca      0.0164552
  44Ca      0.000508923
  46Ti      1.51849e-05
  47Ti      1.3694e-05
  48Ti      0.000135689
  49Ti      9.95764e-06
  50Ti      9.5343e-06
  51V       9.209088e-05
  55Mn      4.623647e-05
  54Fe      0.0007183972
  56Fe      0.01087429
  57Fe      0.0002467372
  58Fe      3.227053e-05
  58Ni      2.662129e-06
  60Ni      9.91618e-07
  61Ni      4.235017e-08
  62Ni      1.329802e-07
  64Ni      3.280212e-07
  63Cu      1.282467e-06
  65Cu      5.545421e-07
  64Zn      3.414323e-06
  66Zn      1.867366e-06
  67Zn      2.679886e-07
  68Zn      1.205877e-06
  85Rb      1.097779e-06
  88Sr      6.816662e-06
  89Y       1.441439e-06
  90Zr      1.584624e-06
  91Zr      3.417629e-07
  92Zr      5.167076e-07
  94Zr      5.124793e-07
```

```
96Zr      8.08394e-08
92Mo      6.930303e-08
94Mo      4.253761e-08
95Mo      7.271993e-08
96Mo      7.558856e-08
97Mo      4.299303e-08
98Mo      1.078814e-07
100Mo     4.240621e-08
204Pb     5.654476e-09
206Pb     9.639215e-08
207Pb     8.796488e-08
208Pb     2.075645e-07
232Th     5.621482e-07
234U      9.504052e-12
235U      1.2625e-09
238U      1.717803e-07

## Material: Borated Concrete rho=3.0942 g/cc
1H        0.013407
10B       0.01
11B       0.04
12C       0.001103
16O       0.043887
27Al      0.0017971
28Si      0.016123
40Ca      0.00183718
44Ca      5.682e-05
54Fe      1.95671e-05
56Fe      0.000306885
57Fe      7.09098e-06
58Fe      9.36544e-07
```

C Concrete Thickness for Prompt Gamma

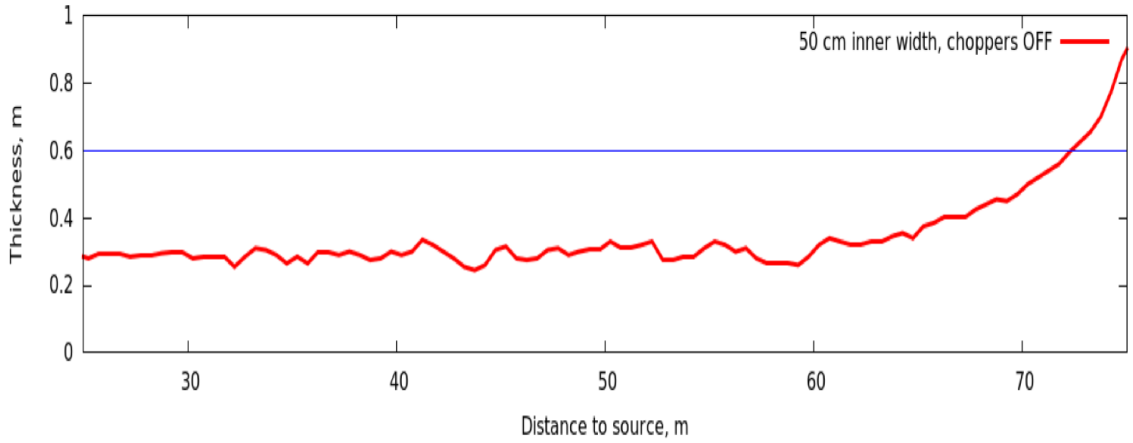

Figure 13: Thickness of the concrete outer layer after 10cm steel necessary to bring the secondary photon dose rate to 1μSv/h, calculated by R. Kolevatov. Picture taken from his slides during IKON15 meeting.

References

[1] T. Sato et al., Particle and Heavy Ion Transport Code System, PHITS, Version 2.52, J. Nucl. Sci. Technol. 50:9,913-923 (2013), DOI:10.1080/00223131.2013.814553.

[2] Tetsuya Kai et al., DCHAIN-SP 2001: High Energy Particle Induced Radioactivity Calculation Code, JAERI-Data/Code-2001-016 (2001) in Japanese.

[3] P. Willendrup, E. Farhi and K. Lefmann, Physica B, 350 (2004) 735.

[4] G. Muhrer and F. Javier, ESS Procedure for Designing Shielding for Safety, ESS-0019931 (2015).

[5] S. Ansell, CombLayer: MCNP(X) Project Builder using C++, https://github.com/SAnsell/CombLayer

[6] S.Kudumovic, Preliminary Design Report - Common Shielding Project, ESS-0484542 (2018).